Journal of Petroleum Science and Engineering 213 (2022) 110376

Contents lists available at ScienceDirect

Journal of Petroleum Science and Engineering

journal homepage: www.elsevier.com/locate/petrol

Aqueous solution of 3-pentanone for enhanced oil production from tight porous media

Mingyuan Wang [a], Gayan A. Abeykoon [b], Francisco J. Argüelles-Vivas [b], Ryosuke Okuno [b,*]

[a] The Research Institute of Petroleum Exploration and Development (RIPED), CNPC, 20 Xueyuan Rd, Haidian, Beijing, 100083, China
[b] Hildebrand Department of Petroleum and Geosystems Engineering, The University of Texas at Austin, 200 E. Dean Keeton Street, Stop C0300, Austin, TX, 78712, USA

ARTICLE INFO

Keywords:
Ketone
Wettability
Imbibition
Improved oil recovery
Tight oil reservoir

ABSTRACT

This paper presents an experimental study of improved oil recovery from fractured tight cores by huff-n-puff of the aqueous solutions of 3-pentanone. The huff-n-puff experiments with different 3-pentanone concentrations were compared. Naturally sulfate-rich brine of low salinity was used as the injection brine.

Results show that the 3-pentanone solution recovered more oil from the matrix than the injection brine alone. The improved oil recovery by 3-pentanone increased to 28.6% of the original oil in place as the 3-pentanone concentration increased up to 2.85 wt% in the injection brine. However, the huff-n-puff experiment with the 1.07-wt% 3-pentanone solution showed the highest efficiency measured by the mass ratio of the produced oil to the injected 3-pentanone, 11.1. That is, an optimal concentration of 3-pentanone appeared to exist.

1. Introduction

Tight oil reservoirs often show low primary recovery factors below 10% with a rapid decline in production rate (Burrows et al., 2020; Clark, 2009; Alharthy et al., 2015; Barba, 2015; Hoffman and Evans, 2016; Alfarge et al., 2017; Hoffman, 2018). Improved oil recovery technologies are important for the exploitation of unconventional reservoirs.

The heterogeneous petrophysical properties are influential in oil recovery from unconventional formations (Ground Water Protection Council and Consulting, 2009; Nelson, 2009). Shale formations are characterized by a small porosity/permeability, diverse minerals, and high total organic content (Mullen, 2010; Alfarge et al., 2017; Alvarez et al., 2018a; Burrows et al., 2020). One major difference in improved oil recovery between the conventional and unconventional reservoirs is that the injectant cannot easily go into the matrix in a tight formation (Burrows et al., 2020). This is because the matrix permeability of tight formations is several orders of magnitude lower than that of the conventional reservoirs (Burrows et al., 2020). The mass transport by advection into the tight rock matrix is significantly slower than that in conventional reservoirs (Cronin et al., 2019). It is important to identify injectants that can transfer efficiently into the matrix.

Since aqueous-solution injection can be operated at a relatively low cost, various aqueous injectants were studied in the literature to improve oil recovery from tight oil reservoirs (Burrows et al., 2020). Aqueous injectants can be used in fracturing fluids, and also for improved oil recovery after the primary depletion (Burrows et al., 2020). Low-salinity water (LSW) and surfactant solutions have been studied by spontaneous imbibition experiments in the literature (Shuler et al., 2011; Wang et al., 2012; Kathel and Mohanty, 2013; Alvarez et al., 2014; Nguyen et al., 2014; Alfarge et al., 2017; Wang et al., 2017; Alvarez and Schechter, 2016; 2017ab; Alvarez et al., 2018a,b; Zeng et al., 2018; Liu et al., 2019).

LSW can improve oil recovery by wettability alteration, desorption of polar oil components from rock surfaces, and mass transfer by osmosis (Austad et al., 2008; Zhang et al., 2013; Li et al., 2016; Valluri et al., 2016; He and Xu, 2017; Teklu et al., 2018; Burrows et al., 2020). Imbibition experiments with LSW showed that the oil recovery factor and rate were low (Burrows et al., 2020). For example, imbibition of water into short cores from Bakken, Wolfcamp, and Eagle Ford required 100–200 h to achieve an ultimate oil recovery of 3–8% OOIP (Alvarez and Schechter, 2016).

Many researchers also studied surfactant solutions for improved oil recovery from shale media. They may improve oil recovery through wettability alteration and interfacial tension (IFT) reduction (Kathel and Mohanty, 2013; Alvarez et al., 2014; Alvarez and Schechter, 2017a,b; Alvarez et al., 2018a,b; Zeng et al., 2018; Liu et al., 2019; Liang et al., 2020). Alvarez et al. (2014) showed that both anionic and non-ionic surfactants improved oil recovery from carbonate shale cores and

* Corresponding author.
E-mail address: okuno@utexas.edu (R. Okuno).

https://doi.org/10.1016/j.petrol.2022.110376
Received 5 December 2021; Received in revised form 26 February 2022; Accepted 3 March 2022
Available online 5 March 2022

siliceous shale cores through wettability alteration. Liu et al. (2019) demonstrated the ability of anionic surfactants to alter the wettability of siliceous shale surfaces. Several studies indicated that the IFT should not reach an ultra-low value for shale IOR with aqueous injectants (Kathel and Mohanty, 2013; Alvarez et al., 2018a; Alvarez and Schechter, 2017a).

In addition to spontaneous imbibition experiments in the lab, aqueous-solution injection was also tested in the field, including fresh or produced water injection and surfactant solution injection (Hoffman and Evans, 2016; Alfarge et al., 2017; Sheng, 2017; Liang et al., 2020). There are mainly two modes of injection used in field pilot tests: continuous injection and huff-n-puff (Burrows et al., 2020). In continuous injection, the aqueous solution is injected into one well and produced from a nearby well (Burrows et al., 2020). In huff-n-puff injection, the aqueous solution is injected, allowed to soak, and produced from the same well (Burrows et al., 2020).

Waterflooding and produced-water huff-n-puff were tested in the Bakken formation with no significant improvement in oil recovery (Hoffman and Evans, 2016). A non-ionic surfactant-based aqueous solution was tested in Middle Bakken (Kazempour et al., 2018). The pilot test was performed in a hydraulically fractured horizontal well after 2.5 years of primary production using huff-n-puff. The shut-in period was four months. An increase in oil production was observed over 1.5 years.

Recently, aqueous solutions of ketone solvent were investigated for improved oil recovery from mixed- or oil-wet media (Wang et al., 2019, 2020 ab; Argüelles-Vivas et al., 2020). 3-Pentanone is a symmetric dialkyl ketone, colorless liquid at standard conditions, and commercially available at a relatively low cost. It is identified in various foods (Nishimura et al., 1989; Idstein and Schreier, 1985; Pet'ka et al., 2012; Bartley and Schwede, 1989; Cavalli et al., 2004; Berlioz et al., 2006).

Two sets of imbibition experiments were performed with reservoir brine (RB) and 1.1-wt% 3-pentanone solution (3pRB) using oil-aged Indiana limestone cores at 347 K (Wang et al., 2019). The experiments demonstrated the ability of 3-pentanone to alter the rock wettability. The Amott index to water was 0.23 for the RB case and 0.76 for the 3pRB case. 3-Pentanone can reduce the polar-polar interaction between oil molecules and the calcite surface through the dipole-ion interaction between the 3-pentanone's carbonyl oxygen and the positively-charged rock surface. 3-Pentanone can not only act as a wettability modifier, but also as a miscible agent. It is miscible with oil, resulting in oil displacement by 3-pentanone through oil swelling and oil viscosity reduction. In addition, the presence of 3-pentanone has essentially no effect on the IFT between the oleic and aqueous phases. Wang et al. (2019) measured IFT values for crude oil and brine solutions with different 3-pentanone concentrations, including 1) crude oil and RB, 2) crude oil and 1.1-wt% 3pRB, and 3) crude oil diluted by 18.6-wt% 3-pentanone and 0.8-wt% 3pRB (Wang et al., 2019). The IFT values for these systems were measured to be close to 11 mN/m at 347 K and atmospheric pressure.

Wang et al. (2020 ab) compared 3-pentanone with a non-ionic surfactant for improved oil recovery from oil-wet fractured cores. The surfactant used was 2-ethylhexanol-4 propylene oxide-15 ethylene oxide (2-EH-4PO-15EO). The contact angle experiments showed that 3-pentanone and 2-EH-4PO-15EO were comparable as wettability modifiers. The IFT between the crude oil and the 1-wt% 2-EH-4PO-15EO solution in reservoir brine was measured to be 0.21 mN/m at 347 K and atmospheric pressure (Wang et al., 2020a). Two sets of dynamic imbibition experiments were performed using fractured limestone cores with continuous injection of 1.1-wt% 3pRB and 1-wt% surfactant solution at 347 K. Results from dynamic imbibition experiments were analyzed by material balance calculation. The 3-pentanone case showed more rapid oil recovery in comparison to the surfactant case. One reason is that 3-pentanone did not affect the interfacial tension (IFT) between the oleic and aqueous phases, unlike the surfactant case. Another reason is that 3-pentanone was more efficient in transferring from a fracture to the surrounding matrix than 2-EH-4PO-15EO.

The previous research on the application of 3-pentanone has demonstrated the improved oil recovery from fractured Texas Cream and Indiana limestone cores in continuous injection. In this research, 3-pentanone was tested for the first time with fractured tight cores in huff-n-puff. Also, unlike the previous studies, different concentrations of 3-pentanone were tested.

The tight cores used in this research are rich in calcite, which is one of the common minerals in some major tight formations. For example, rock samples from the Eagle Ford are consistently calcite-dominated, with the calcite concentrations ranging from 40-wt% to 83-wt% (Alvarez and Schechter, 2016; Zeng et al., 2020; Chen and Schechter, 2021). Some samples from Wolfcamp are also calcite-dominated. For example, one sample from Alhashim et al. (2019) contains 78-wt% calcite and 15-wt% quartz.

In the next section, the materials and methods are presented. Section 3 presents results and discussions of experiments. Section 4 gives the main conclusions.

2. Materials and methods

This section presents the materials and experimental methods for this study. The main experimental data were obtained through contact-angle experiments, and three sets of huff-n-puff experiments with 3-pentanone solutions in injection brine (3pIB) at different concentrations at 338 K.

Median lethal dose, LD_{50}, is used to describe the toxicity of 3-pentanone in comparison to that of methane, a common component in hydrocarbon reservoirs. LD_{50} decreases with increasing toxicity. LD_{50} Mouse (intravenous) is 513 mg/kg for 3-pentanone and 440 mg/kg for methane (European Chemicals Bureau, 2007; Vacher et al., 1973; PubChem). One of the parameters to evaluate the environmental safety of chemicals is their flash point. The flash point of 3-pentanone is 286 K, while that of methane is 85 K (Daubert and Danner, 1985; CAMEO Chemicals).

2.1. Crude oil and injection brine properties

A crude oil sample from a shale oil reservoir in Texas was used in this research. This crude oil is different from the crude oil used in the previous studies by Wang et al. (2019, 2020 ab). Table 1 summarizes properties of the crude oil sample. Table 2 presents the composition of the crude oil sample measured by gas chromatography. The molecular weight of the crude oil sample was measured to be 239 g/mol. The reservoir temperature is 338 K. Figs. 1 and 2 give the oil densities and viscosities measured at different conditions. Table 3 shows the ionic composition of injection brine (IB) (7655 ppm) based on the relevant field-operation data. The IB composition is substantially different from that of the reservoir brine in the previous studies by Wang et al. (2019, 2020 ab). IB has a low salinity, but is rich in sulfate (2000 ppm); IB by itself can make rock surfaces less oil-wet, as will be shown in Section 3.1. The IB density was 999.0 kg/m^3 at 338 K and atmospheric pressure. The solubility limit of 3-pentanone in IB was measured to be 2.85 wt% at 338 K and atmospheric pressure.

Table 1
Properties of the crude oil sample used in this research. Oil densities and viscosities at high pressures are presented in Figs. 1 and 2.

Molecular weight, g/mol		239
Density, kg/m^3		820.0 (at 295 K)
		780.0 (at 338 K)
Viscosity, cp		1.09 (at 338 K)
SARA, wt%	Saturates	86.1
	Aromatics	9.8
	Resins	<4.3
	Asphaltenes (pentane insoluble)	<0.1
Acid number, mg-KOH/g-oil		0.02

Table 2
The composition of the crude oil measured by gas chromatography. The molecular weight of the crude oil sample was measured to be 239 g/mol.

Component	Mass fraction
CH_4	<0.0001
C_2H_6	<0.0001
C_3H_8	0.0004
C_4H_{10}	0.0032
C_5H_{12}	0.0126
C_6H_{14}	0.0265
C_{7+}	0.9573

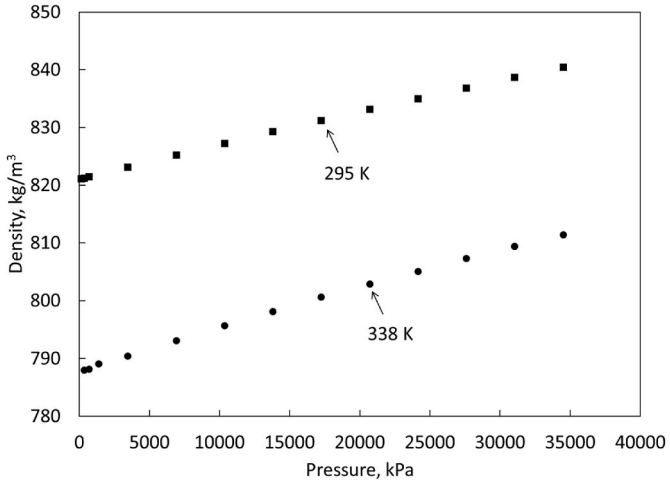

Fig. 1. Densities of crude oil at room temperature (295 K) and reservoir temperature (338 K).

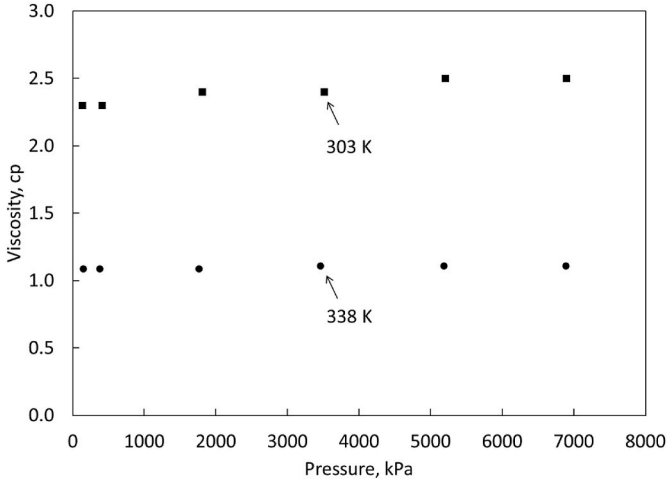

Fig. 2. Viscosities of crude oil at room temperature (303 K) and reservoir temperature (338 K).

2.2. Contact-angle experiments

The contact-angle experiments were performed on oil-aged calcite surfaces in 3pIB at different concentrations at 338 K. Calcite is one of the major minerals in some major tight formations, and calcite surfaces can represent an oil-wet state by aging them in oil. We did not use tight rock samples to perform the contact-angle experiment because contact angles measured on porous media are subject to the complexities, such as surface roughness and heterogeneity, which affect the representativeness of the contact angles (Anderson, 1986). The polished calcite pieces were first cleaned with deionized water and air-dried. Then, they were aged in RB for 1 day at 338 K and air-dried. After that, the calcite pieces were aged in crude oil with an acid number of 0.17 mg-KOH/g-oil for at least 3 weeks at 338 K. They were then aged in heavy oil with an acid number of 8.08 mg-KOH/g-oil for at least 4 weeks at 338 K to ensure that the calcite surfaces were oil-wet. These crude oils used for aging have higher acid numbers than the crude oil described in Section 2.1. The calcite pieces were taken out of the oil after aging. Any excess oil was carefully removed from the surfaces by gently wiping the surface with KIMTECH delicate task wipers.

Table 3
Composition of the injection brine (IB) used in this research (7655.34 ppm). The density of IB was measured to be 999.0 kg/m^3 at 338 K and atmospheric pressure. IB is naturally sulfate-rich brine of low salinity and available for injection near a field-operation site.

Cations	ppm	Anions	ppm
Ca^{2+}	792.99	HCO_3^-	97.76
Mg^{2+}	348.29	SO_4^{2-}	2000.00
Na^+	1380.47	Cl^-	3023.91
Sr^{2+}	11.92		

Before the contact-angle measurements, IB and 3pIB at different concentrations (0.5 wt%, 1.0 wt%, 2.0 wt%, and 2.85 wt%) were prepared and degasified at 338 K. Then, an oil-aged calcite piece was placed inside a glass chamber for each solution. An oil droplet was placed on the bottom surface of each calcite piece. The oil used in this step was the crude oil described in Section 2.1. Since 3-pentanone may have been partly evaporated during this process, a sample of the 3-pentanone solution was taken from each solution to quantify the 3-pentanone concentration after this process by the ^{1}H NMR method. The 3-pentanone concentrations in 3pIB were measured to be 0.39 wt%, 0.77 wt%, 1.39 wt%, and 2.14 wt%. The glass chamber was then tightly closed, and a photo of each oil droplet was taken to quantify the initial contact angle. The glass chamber was then placed inside an oven at 338 K. After calcite pieces were submerged in solutions for one day, there were gas bubbles on the calcite surfaces, which were merged with oil droplets. A new oil droplet was then placed on the bottom surface of each calcite surface after all gas bubbles were removed. The gas bubbles were removed by slightly shaking the calcite piece with a tweezer inside the solution. The tweezer was carefully cleaned with hexane and deionized water before using it for this procedure. Photos of oil droplets were taken every day. Onscreen protractor software was used to measure the contact angles on both sides of each oil droplet. The average and standard deviation of contact angle data were then calculated.

The contact-angle experiments in this research are different from the previous ketone studies by Wang et al. (2019, 2020a). The previous studies presented contact angles in reservoir brine and 3-pentanone solution in reservoir brine. This research presents contact angles in the IB and 3pIB. This is the first time contact angle values with 3pIB were measured and reported. Also, unlike the previous studies, different concentrations of 3-pentanone were tested in the contact-angle experiments.

2.3. Huff-n-puff experiments

Three huff-n-puff experiments were performed at 338 K with Wolfcamp outcrop cores using 3pIB at different concentrations: Case 1 with 0.56-wt% 3pIB, Case 2 with 1.07-wt% 3pIB, and Case 3 with 2.85-wt% 3pIB. This section describes the procedures for preparing tight cores and huff-n-puff experiments.

Wolfcamp outcrop cores (Kocurek Industries Inc.) were used in this research. Table 4 presents the mineral composition of the cores, which was measured by X-ray diffraction analysis (XRD). Because of their ultra-low permeability, the Wolfcamp outcrop cores were cut into small

Table 4
Mineral composition of Wolfcamp outcrop cores used in this research measured by XRD method. The cores are calcite rich. The TOC of the Wolfcamp outcrop sample from Kocurek Industries Inc. was reported to be 0.21 wt% (Zeng et al., 2020). The outcrop sample used in this research was from the same company with a similar mineral composition as Zeng et al. (2020); therefore, the TOC was expected to be similar to the cores used in Zeng et al. (2020).

Mineral	Concentration, wt%
Quartz	2.3
Calcite	96.7
Dolomite	0.6
Feldspar	<0.5
Pyrite	0.0
Clays	0.0

pieces with 0.0127 m in length and 0.0381 m in diameter before being saturated with any fluids. In this research, the core pieces were saturated only by crude oil (Table 1) at room temperature. They were placed in an accumulator, which was evacuated for at least 24 h. Then, the crude oil was transferred into the accumulator, and the pressure inside the accumulator was set at 66,190 kPa for 1 week. Some of the core pieces were aged in the crude oil for more than four months because of the lab shut-down owing to the COVID-19 pandemic. The mass of each core piece was measured before and after the saturation and/or the aging to quantify the oil volume in the core. This volume was assumed to be accessible pore volume (PV). Before measuring the mass of the core pieces, any excess oil was carefully removed from the surfaces of the core pieces by gently wiping the surface with KIMTECH nitrile exam gloves. The balance used was Mettler Toledo ML104T analytical balance with a capacity of 120 g and an accuracy of 0.0001 g. The mass of each core piece was measured at least twice either before or after the saturation (and/or aging), to ensure the repeatability of the measurement. We did not use a porosimeter to measure the actual pore volume because the accessible pore volume was important for quantifying oil recovery and mass balance calculation. The actual pore volume is usually larger than the accessible pore volume, as explained in the next paragraph. Table 5 presents the properties of the core pieces, including the length and accessible pore volume.

The accessible porosity calculated from the accessible pore volume in Table 5 ranged from 0.08% to 0.71%, with an average value of 0.45%, which is deemed reasonable based on the literature. Tovar et al. (2018) measured the actual porosities of 11 reservoir core samples from the Wolfcamp by using a gas expansion pycnometer after the core samples were cleaned with toluene and methanol. The actual porosities of the samples ranged from 5.94% to 10.30%. Then, the core samples were re-saturated with dead crude oil using a similar method as in this research. The accessible porosities ranged from approximately 1.52%–8.76%. Tovar et al. (2018) explained that the accessible porosities were much smaller than the actual porosities because large oil molecules could not access micropores in the shale matrix, or some pore throats were too small for oil molecules to pass.

Instead of using reservoir core samples as Tovar et al. (2018), this research used outcrop core samples. One difference between outcrop and reservoir core samples is their total organic content (TOC), which affects the porosity. The TOC of the Wolfcamp outcrop sample from Kocurek Industries Inc. was reported to be 0.21 wt% (Zeng et al., 2020). The Wolfcamp outcrop sample used for this research was from the same company with a similar mineral composition as Zeng et al. (2020). The TOC of the cores used in this research likely had a similar value as that in Zeng et al. (2020). In comparison, the TOC of reservoir core samples ranged from 3.0 wt% to 5.7 wt%, which was larger than that of the outcrop sample (Alvarez and Schechter, 2016). Slatt et al. (2018) reported a positive correlation between porosity and TOC. For example, as

Table 5
Properties of the core pieces. Core pieces #1-#10 were used for Case 1 (with 0.56-wt% 3pIB). Core pieces #11-#20 were used for Case 2 (with 1.07-wt% 3pIB). Core pieces #21-#30 were used for Case 3 (with 2.85-wt% 3pIB). The 3rd and 4th columns respectively refer to the accessible pore volume before and after an artificial fracture was made for each core piece. The cutting process lost a certain mass; as a result, the accessible pore volume of each core piece decreased after the cutting process.

Core piece #	Length, m	Accessible pore volume before cutting, m^3	Accessible pore volume after cutting, m^3	Aging time, week	Accessible porosity, %
1	0.0101	3.56×10^{-8}	3.49×10^{-8}	21	0.31
2	0.0118	8.49×10^{-8}	8.24×10^{-8}	21	0.63
3	0.0102	7.20×10^{-8}	7.02×10^{-8}	21	0.62
4	0.0104	6.25×10^{-8}	6.01×10^{-8}	21	0.53
5	0.0097	0.90×10^{-8}	0.88×10^{-8}	21	0.08
6	0.0111	7.08×10^{-8}	6.89×10^{-8}	21	0.56
7	0.0089	7.17×10^{-8}	6.92×10^{-8}	21	0.71
8	0.0108	6.71×10^{-8}	6.53×10^{-8}	21	0.55
9	0.0109	2.81×10^{-8}	2.72×10^{-8}	21	0.23
10	0.0111	4.83×10^{-8}	4.69×10^{-8}	21	0.38
11	0.0100	5.25×10^{-8}	5.11×10^{-8}	4	0.46
12	0.0120	8.10×10^{-8}	7.83×10^{-8}	4	0.59
13	0.0100	5.30×10^{-8}	5.16×10^{-8}	4	0.46
14	0.0100	3.49×10^{-8}	3.40×10^{-8}	4	0.31
15	0.0100	6.66×10^{-8}	6.49×10^{-8}	4	0.58
16	0.0115	7.27×10^{-8}	7.10×10^{-8}	4	0.55
17	0.0100	5.37×10^{-8}	5.23×10^{-8}	4	0.47
18	0.0105	6.64×10^{-8}	6.45×10^{-8}	4	0.55
19	0.0093	4.86×10^{-8}	4.74×10^{-8}	4	0.46
20	0.0110	6.10×10^{-8}	5.95×10^{-8}	4	0.49
21	0.0102	5.37×10^{-8}	5.20×10^{-8}	21	0.46
22	0.0113	6.59×10^{-8}	6.42×10^{-8}	21	0.51
23	0.0113	4.22×10^{-8}	4.11×10^{-8}	21	0.33
24	0.0107	3.76×10^{-8}	3.64×10^{-8}	21	0.31
25	0.0096	3.98×10^{-8}	3.86×10^{-8}	21	0.36
26	0.0111	7.05×10^{-8}	6.85×10^{-8}	21	0.56
27	0.0122	4.05×10^{-8}	3.96×10^{-8}	21	0.29
28	0.0110	4.10×10^{-8}	4.01×10^{-8}	21	0.33
29	0.0106	4.98×10^{-8}	4.85×10^{-8}	21	0.41
30	0.0109	4.76×10^{-8}	4.65×10^{-8}	21	0.38

TOC increased from 1 wt% to 5 wt%, the gas-filled porosity increased from approximately 1.9%–3.9% (Slatt et al., 2018). Therefore, it is expected that the porosity of samples used in this research was smaller than that in Tovar et al. (2018). The permeabilities of the core samples were not measured; as explained in Tovar et al. (2018), it is difficult to inject any significant amount of low viscosity gas within a reasonable time frame for the shale matrix. Alvarez and Schechter (2017b) estimated the permeability of Wolfcamp shale samples by the mercury injection capillary pressure technique. They reported that the permeability of Wolfcamp reservoir shale samples ranged from 100 nD to 250 nD.

An artificial fracture was made for each core piece along the longitudinal axis by an electric saw. Polytetrafluoroethylene (PTFE) spacers with 0.0010 m in width and 0.1270 m in length were used to maintain the artificial fracture aperture (Mejia, 2018). A PTFE tube was then used to wrap the core halves and the PTFE spacer in the artificial fracture. For each core assembly, the longitudinal fracture is referred to as "propped fracture," and the transverse fractures as "unpropped fractures" in this paper. Fig. 3 shows the assembled core pieces, which were placed inside a horizontally-oriented core holder with the propped fracture vertically oriented. Then, the core assembly was tightened from both ends to make sure the core pieces were in close contact with one another; that is, the volume of the unpropped fractures was minimized. Table 6 summarizes the properties of the assembled core pieces used for three huff-n-puff experiments. Core pieces #1–10 were used for Case 1, #11–20 for Case 2, and #21–30 for Case 3. The objective of using the artificial fracture in the experiments was to test the oil recovery from the surrounding matrix through wettability alteration. The propped fracture

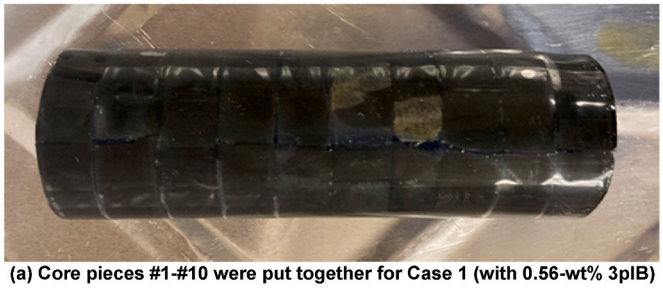

(a) Core pieces #1-#10 were put together for Case 1 (with 0.56-wt% 3pIB)

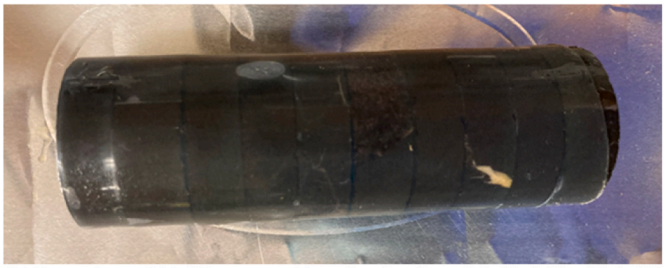

(b) Core pieces #11-#20 were put together for Case 2 (with 1.07-wt% 3pIB)

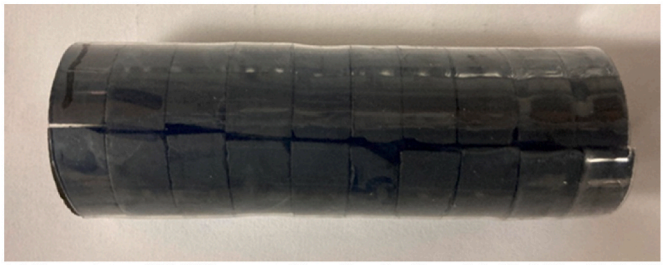

(c) Core pieces #21-#30 were put together for Case 3 (with 2.85-wt% 3pIB)

Fig. 3. Assembled cores for three huff-n-puff experiments.

Table 6
Properties of core pieces #1–10 for case 1, #11–20 for case 2, and #21–30 for case 3.

	Core pieces #1–10 (Case 1)	Core pieces #11–20 (Case 2)	Core pieces #21–30 (Case 3)
Oil volume in matrix at 338 K and atmospheric pressure, m^3	5.34×10^{-7}	5.75×10^{-7}	4.75×10^{-7}
Pressure drop along the core at 500 cm^3/h, kPa	3.51630	2.95030	4.13690
Overburden pressure, kPa	11133	6996	6789
The propped fracture aperture, m	0.1122×10^{-3}	0.1192×10^{-3}	0.1076×10^{-3}
The propped fracture permeability, darcy	1059	1196	1022
The propped fracture volume, m^3	0.4489×10^{-6}	0.4737×10^{-6}	0.4464×10^{-6}

was not created inside the core-holder, because it would be difficult to quantify the shape and volume of the propped fracture.

Fig. 4 shows the experimental set-up for the huff-n-puff experiments. It consisted of in-house accumulators for crude oil, IB, and 3pIB, a pump (Teledyne Isco 100 DX), a Hassler-type core-holder (Phoenix Instruments, Serial # UTPT-HAS-1.5 × 12-10k-56), a hydraulic manual pump (ENERPAC P-391) to maintain the overburden pressure of the core-holder, a pressure gauge (OMEGA PX459-2.5KGI-EH), graduating cylinders (Thermo Scientific with a capacity of 15 cm^3), and a Blue M oven (model DC-1406-F-PM-GOP). After the experimental set-up was assembled, the oven temperature was increased to 338 K. Then, the core-holder was evacuated for 10 s to remove any gas inside the fractures. The fracture permeability was measured by injecting crude oil at 500 cm^3/h under a certain overburden pressure. The overburden pressure was adjusted so that all core assemblies had similar propped fracture aperture. Table 6 gives the overburden pressure values and the pressure drops along the cores. The overburden pressures were different for different core assemblies likely because the propped fracture surface had different degrees of roughness among the three core assemblies. Each core assembly was put together by ten core pieces. Among ten core pieces, the fracture shapes were slightly different from each other, which caused the roughness along the propped fracture in the core assembly.

The method provided by Mejia (2018) was used to quantify the propped fracture apertures and permeabilities. The fracture aperture was calculated by

$$b = (3\pi d k_e)^{\frac{1}{3}} \quad (1)$$

where b is the fracture aperture, d is the diameter of the core, and k_e is the effective oil permeability of the fractured core with the unit m^2, which was calculated by

$$k_e = (Q\mu_o L) / (A\Delta P) \quad (2)$$

where Q is the flow rate of the crude oil, μ_o is the crude oil viscosity at reservoir temperature and atmospheric pressure, L is the length of the core assembly, A is the cross-sectional area of the core assembly, and ΔP is the pressure drop along the core assembly. The fracture permeability was calculated by

$$k_f = b^2/12. \quad (3)$$

Table 6 also presents the values of fracture apertures and permeabilities. The propped fracture aperture in this research ranged from 0.1076×10^{-3} m to 0.1192×10^{-3} m. These values are within the range of the propped fracture aperture reported in the literature. For example, Mejia (2018) used the same method of preparing a propped fracture. The propped fracture aperture reported in Mejia (2018) ranged from 0.026×10^{-3} m to 0.17×10^{-3} m.

As shown in Table 6, the propped fracture volumes were similar to the oil volume in the matrix in this research. The propped fracture volume was important for performing the huff-n-puff experiment, as well as mass balance calculation. It was used to determine the amount of 3pIB to be injected during each cycle of 3pIB huff-n-puff. The amount of 3p injected was then used in the mass balance calculation. In comparison, the properties of the unpropped fractures did not affect the experimental procedure; therefore, properties of the unpropped fractures were not shown in Table 6.

There were four stages during huff-n-puff experiments: one IB flooding period and three cycles of 3pIB huff-n-puff. During the IB flooding period, IB was injected at 0.6 cm^3/h for 8 h, and then the system was shut-in for at least 10 h. After that, IB was injected at 0.6 cm^3/h until the water-cut was higher than 0.99. The purpose of the IB flooding was to recover the crude oil inside the fracture so that the produced oil during the following 3pIB huff-n-puff was from the matrix. During each cycle of 3pIB huff-n-puff, the 3pIB was injected to fill the propped fracture volume. Then, the system was shut-in for at least 8 h. After that, IB was injected at 6 cm^3/h until there was no oil production. This step was used to make sure all the produced oil inside the fracture and the pipes was displaced to the outlet.

Plastic graduating cylinders were used to receive the produced fluids at room temperature. The 3-pentanone concentrations in the produced fluids were measured by the ^1H NMR method during the 3pIB huff-n-puff. The concentration data were used to correct oil-recovery results for 3-pentanone solubility and perform material balance calculations. For each graduating cylinder with the produced aqueous and oleic phases, the total mass was measured first. Then, the aqueous phase in the graduating cylinder was carefully transferred to another graduating cylinder. After this step, the graduated cylinder was double-checked to see if all the aqueous phase was transferred. If there was any aqueous

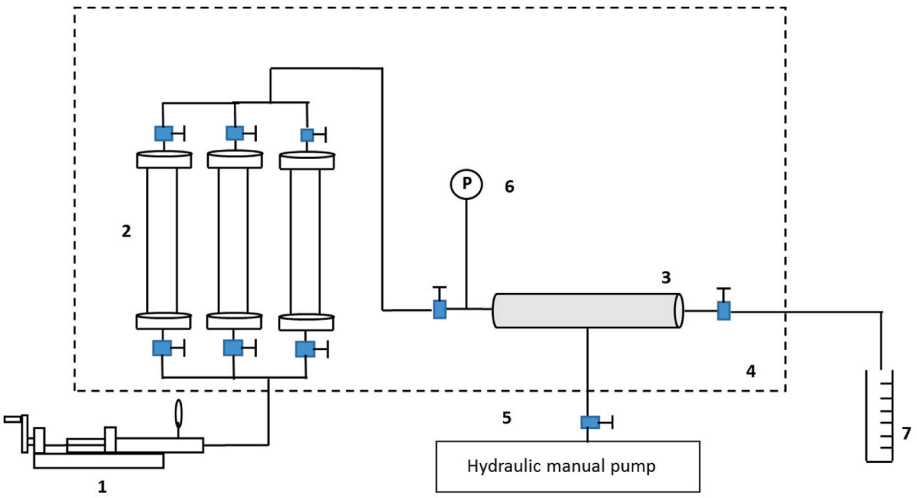

Fig. 4. Schematic of the experimental set up for huff-n-puff experiments. The pressurization pump was TELEDYNE ISCO 100 DX pump. The hydraulic manual pump was ENERPAC P-391 pump. The pressure gauge was from OMEGA (PX459-2.5KGI-EH). The Hassler type core holder was from Phoenix Instruments (Serial # UTPT-HAS-1.5 × 12-10k-56). The oven was a Blue M oven (DC-1406-F-PM-GOP). Accumulators were made in-house. The graduating cylinder was from Thermo Scientific, with a capacity of 15 cm^3. (For interpretation of the references to color in this figure legend, the reader is referred to the Web version of this article.)

phase left, the transfer procedure was repeated until all the aqueous phase was transferred. After that, the mass of the graduating cylinder with the oleic phase inside was measured. The difference between the mass of the graduating cylinder with and without the oleic phase was the mass of the recovered oleic phase. Then, the recovered oil volume was calculated by using the mass of the recovered oleic phase, the 3-pentanone concentration in the recovered oleic phase, and the crude oil density. The balance used was Mettler Toledo ML104T analytical balance with an accuracy of 0.0001 g.

The efficiency of 3-pentanone was quantified by M_{P2}/M_{I3}, in which M_{P2} is the mass of produced oil, and M_{I3} is the mass of injected 3-pentanone. The greater the M_{P2}/M_{I3} value, the higher the efficiency of 3-pentanone in terms of improving oil recovery.

3. Results and discussions

This section presents the main results of the contact-angle and three huff-n-puff experiments with 3pIB at different 3-pentanone concentrations. The purposes of these experiments were to quantify the improved oil recovery from tight cores by 3-pentanone and to investigate the effect of 3-pentanone concentration on the improved oil recovery from tight cores.

3.1. Contact-angle experiments

As described in Section 2.2, contact angles were measured in IB and 3pIB at 0.39 wt%, 0.77 wt%, 1.39 wt%, and 2.14 wt% at 338 K. Figs. 5 and 6 present photos of oil droplets at the initialization of the experiments and 3 days after the oil-aged calcite pieces were immersed in the solutions at 338 K and atmospheric pressure. The oil-aged calcite surface was oil-wet initially. The initial average contact angle in IB was 113.05°. After 3 days, the average contact angle was 87.09° in IB. IB by itself was able to make rock surface less oil-wet likely because this low salinity water was rich in sulfate (Table 2), which reduced the interaction between oil components and rock surfaces.

Fig. 7 compares the contact angles in different solutions after 3 days. The contact angle only slightly decreased by 2.03° when the 3-pentanone concentration increased from 0 wt% to 0.39 wt%. The 3-pentanone effectively reduced the contact angle by 10.17° when the 3-pentanone concentration increased from 0.39 wt% to 0.77 wt%. However, as the 3-pentanone concentration increased from 0.77 wt% to 2.14 wt%, the contact angle only decreased by 9.27°. The calcite surface became more water-wet as the 3-pentanone concentration increased; however, the wettability became less sensitive to the 3-pentanone concentration as it increased above 0.77 wt%.

3.2. Huff-n-puff experiments

The experimental data of the huff-n-puff experiments are summarized in this section and discussed in Section 3.3. Table 7 presents the results with 0.56-wt% 3pIB. Oil recovery was observed after each cycle of the 3pIB huff-n-puff. The oil recovery was 2.6% of the original oil in the matrix (OOIM) after the 1st cycle of 3pIB huff-n-puff, 7.5% of OOIM after the 2nd cycle, and 10.2% of OOIM after the 3rd cycle. $M_{P2}/M_{I3}$was calculated on the cumulative basis, for which the time interval started from the 1st cycle of 3pIB huff-n-puff. M_{P2}/M_{I3} was 4.38 after the 1st cycle, 6.25 after the 2nd cycle, and 5.66 after the 3rd cycle.

Table 8 presents the results with 1.07-wt% 3pIB. Oil recovery was observed only after the 1st cycle of the 3pIB huff-n-puff. The oil recovery was 12.5% of OOIM after the 1st cycle of 3pIB huff-n-puff. M_{P2}/M_{I3} was 11.11 after the 1st cycle.

Table 9 presents the results with 2.85-wt% 3pIB. Oil recovery was also observed only after the 1st cycle of the 3pIB huff-n-puff. The oil recovery was 28.6% of OOIM. M_{P2}/M_{I3} was 8.18 after the 1st cycle.

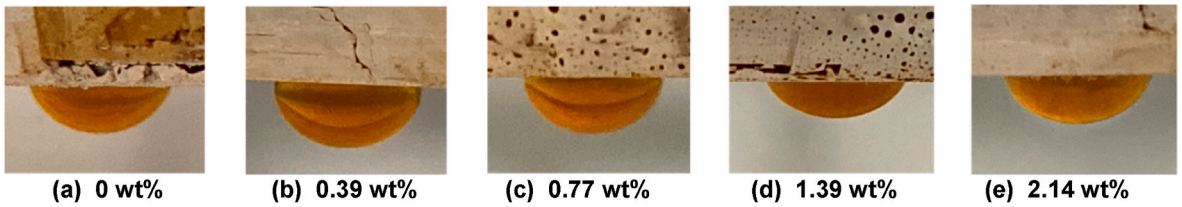

Fig. 5. Photos of oil droplets at the initialization of the experiments. The oil-aged calcite surfaces were intermediate-wet to oil-wet initially. The average contact angle was 113.05° for IB, 90.55° for 0.39-wt% 3pIB, 100.09° for 0.77-wt% 3pIB, 123.91° for 1.39-wt% 3pIB, and 112.03° for 2.14-wt% 3pIB.

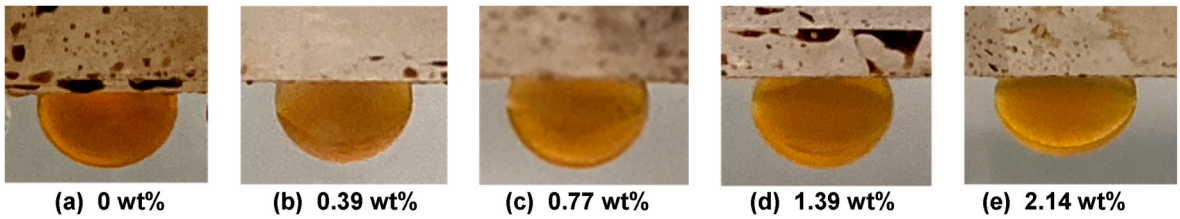

Fig. 6. Photos of oil droplets at 3 days after the oil-aged calcite pieces were immersed in the solutions at 338 K and atmospheric pressure. IB (shown as "0 wt%") by itself made rock surface less oil-wet. The calcite surface became more water-wet as the 3-pentanone concentration increased; however, the wettability alteration was less sensitive to the change in 3-pentanone concentration when the 3-pentanone concentration was high. The average contact angle was 87.09° for IB, 85.06° for 0.39-wt% 3pIB, 74.89° for 0.77-wt% 3pIB, 68.71° for 1.39-wt% 3pIB, and 65.63° for 2.14-wt% 3pIB.

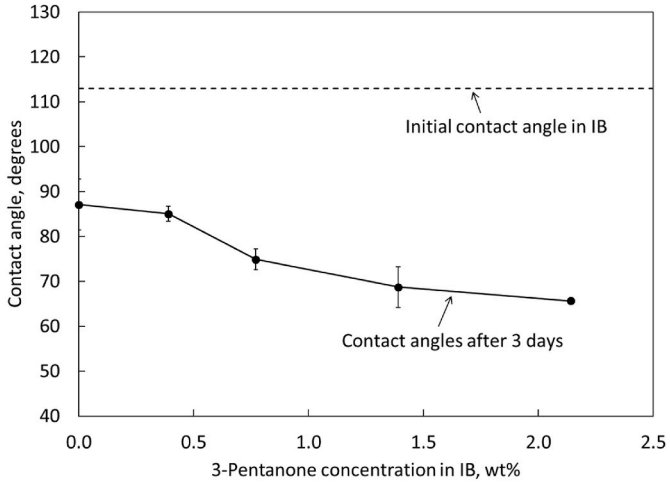

Fig. 7. Contact angles measured for IB at initialization of the experiment and for IB and 3pIB at different concentrations 3 days after the oil-aged calcite pieces were immersed in the solutions at 338 K and atmospheric pressure. Standard deviations of contact angles are shown as the error bars in the figure. IB by itself made rock surface less oil-wet. The calcite surface became more water-wet as the 3-pentanone concentration increased; however, the sensitivity of contact angle to the 3-pentanone concentration varied.

Table 7
Results of the huff-n-puff experiment with 0.56-wt% 3pIB (Case 1).

	Improved oil recovery (OOIM)	Mass of injected 3-pentanone (M_{I3}), g	Mass of oil recovered (M_{P2}), g	M_{P2}/M_{I3}
After first cycle	2.6%	0.0025	0.0110	4.38
After second cycle	7.5%	0.0050	0.0314	6.25
After third cycle	10.2%	0.0075	0.0426	5.66

Table 8
Results of the huff-n-puff experiment with 1.07-wt% 3pIB (Case 2).

	Improved oil recovery (OOIM)	Mass of injected 3-pentanone (M_{I3}), g	Mass of oil recovered (M_{P2}), g	M_{P2}/M_{I3}
After first cycle	12.5%	0.0051	0.0562	11.11
After second cycle	12.5%	0.0101	0.0562	5.56
After third cycle	12.5%	0.0152	0.0562	3.70

Table 9
Results of the huff-n-puff experiment with 2.85-wt% 3pIB (Case 3).

	Improved oil recovery (OOIM)	Mass of injected 3-pentanone (M_{I3}), g	Mass of oil recovered (M_{P2}), g	M_{P2}/M_{I3}
After first cycle	28.6%	0.0130	0.1062	8.18
After second cycle	28.6%	0.0260	0.1062	4.09
After third cycle	28.6%	0.0390	0.1062	2.73

3.3. *Effect of 3-pentanone concentration on improved oil recovery*

The three huff-n-puff experiments demonstrated that 3pIB increased the oil recovery from the tight rock matrix more than IB alone. Figs. 8 and 9 compare the improved oil recovery and M_{P2}/M_{I3} from different cases. The improved oil recovery increased with increasing 3-pentanone concentration. The huff-n-puff experiment with 2.85-wt% 3-pentanone solution showed the highest improved oil recovery; however, the huff-n-puff experiment with 1.07-wt% 3-pentanone solution showed the highest M_{P2}/M_{I3} value. An optimal concentration in terms of efficiency of 3-pentanone gives the highest value of M_{P2}/M_{I3} for a given volume of the rock.

Similar observations were made from the previous dynamic imbibition experiments with Indiana and Texas Cream limestone cores (Wang et al., 2020a; Argüelles-Vivas et al., 2020). Wang et al. (2020b) showed the vertical dynamic imbibition with the 1.1-wt% 3-pentanone solution

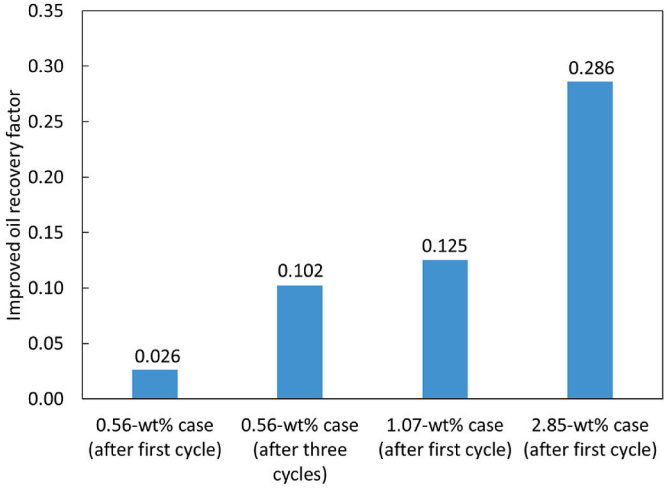

Fig. 8. Improved oil recovery factors for different cases of the huff-n-puff experiments. Improved oil recovery increased with increasing 3-pentanone concentration. Huff-n-puff experiments with 2.85-wt% 3pIB showed a much greater improved oil recovery by 3-pentanone than the other cases.

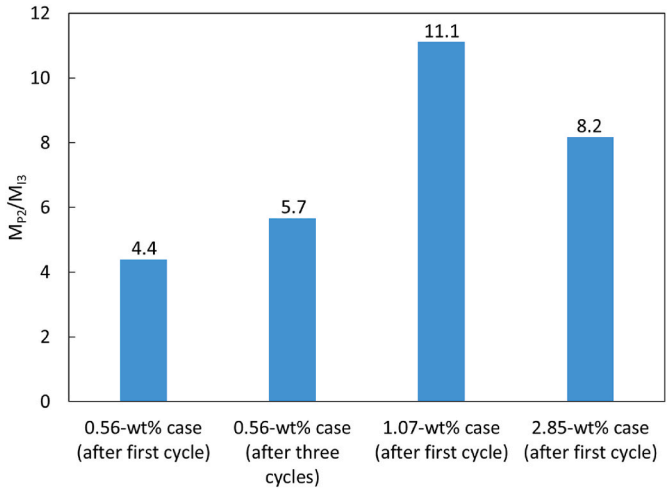

Fig. 9. M_{P2}/M_{I3} values for different cases of the huff-n-puff experiments. The huff-n-puff experiment with 1.07-wt% 3-pentanone solution showed the highest M_{P2}/M_{I3} value. The result indicates that there is an optimal concentration in terms of efficiency of 3-pentanone, which gives the highest value of M_{P2}/M_{I3} for a given volume of the rock.

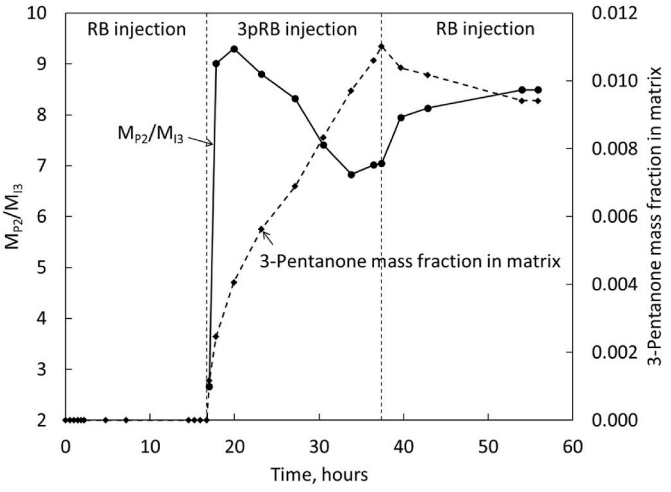

Fig. 11. 3-Pentanone mass fraction in the matrix and M_{P2}/M_{I3} for the vertical dynamic imbibition with 3pRB using Indiana limestone cores (Wang et al., 2020b). As 3pRB was continuously injected into the fracture, M_{P2}/M_{I3} increased first, then decreased. This indicates that there should be an optimal amount of 3-pentanone in the matrix that gives the highest value of M_{P2}/M_{I3}.

in reservoir brine (3pRB) using an Indiana limestone core. There were three stages in their dynamic imbibition experiment: reservoir brine (RB) injection stage, 3pRB injection stage, and chase RB injection stage. Figs. 10 and 11 present oil recovery, 3-pentanone mass fraction in the matrix, and M_{P2}/M_{I3} for the vertical dynamic imbibition with 3pRB (Wang et al., 2020b). M_{P2}/M_{I3} were calculated on a cumulative basis, for which the time interval started at the beginning of the 3pRB injection stage. As 3pRB was continuously injected into the fracture, the 3-pentanone amount in the matrix and oil recovery continuously increased. However, M_{P2}/M_{I3} increased first, and then decreased. Similar observations were also made from other cases in Wang et al. (2020b) and Argüelles-Vivas et al. (2020). Huff-n-puff experiments with tight cores and dynamic imbibition experiments with limestone cores indicate that there should be an optimal amount of 3-pentanone in the matrix that gives the highest value of M_{P2}/M_{I3}.

Why there is an optimal amount of 3-pentanone in the matrix is likely related to the capillary pressure change in response to wettability alteration. That is, as the 3-pentanone concentration increases, the matrix becomes more water-wet; thus, capillary pressure tends to increase. However, capillary pressure may have become less sensitive to the change in 3-pentanone concentration when the 3-pentanone concentration is high under a strongly water-wet state. Contact-angle results shown in Section 3.1 are consistent with this hypothesis.

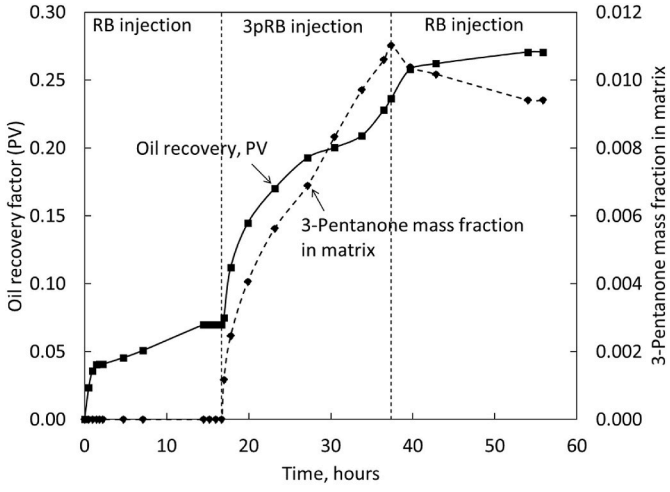

Fig. 10. Oil recovery factor and 3-pentanone mass fraction in the matrix for the vertical dynamic imbibition with 3pRB using Indiana limestone cores (Wang et al., 2020b). Oil recovery factors are given as a fraction of PV. As 3pRB was continuously injected into the fracture, the 3-pentanone amount in the matrix and oil recovery both continuously increased.

Among many other factors, wettability alteration and swelling are the main mechanisms that should have affected the observed efficiencies of 3-pentanone, M_{P2}/M_{I3}, and oil recovery factors. The oil recovery factor increases when 3-pentanone increases its impact on rock wettability with increasing concentration, as shown in Figs. 5 and 6. As the concentration of 3-pentanone increases above an optimal value, however, rock wettability tends to become less sensitive. Then, the mass transfer of 3-pentatone from water to oil causes the oil swelling that expels oil from the rock matrix and, therefore, continues to increase the oil recovery factor. For field applications of the aqueous solution of 3-pentanone, an optimal injection scheme would maximize the contribution from rock wettability alteration, instead of that from oil swelling.

There was one difference between dynamic imbibition experiments using limestone cores and huff-n-puff experiments using tight cores. For huff-n-puff experiments with 1.07-wt% and 2.85-wt% 3pIB, oil recovery was only observed after the first cycle of huff-n-puff; further injection of the 3pIB in the 2nd and 3rd cycles recovered a negligible amount of oil. In comparison, Fig. 10 shows that as 3pRB was continuously injected into the fracture, the amount of 3-pentanone in the matrix and oil recovery continuously increased. Apparently, the capillary forces alone did not let 3-pentanone go further into the matrix in the 2nd and 3rd cycles of 3pIB huff-n-puff. It is desirable to have stronger driving forces to push 3-pentanone into the matrix, for example, by soaking at higher pressure.

4. Conclusions

This paper presented the first study of 3-pentanone as a wettability modifier for improved oil recovery from tight cores in huff-n-puff experiments. Different concentrations of 3-pentanone were tested to see the effect on improved oil recovery. The brine used for the 3-pentanone solutions was sulfate-rich low-salinity water that was available for injection. The main conclusions are as follows:

a. The contact angle experiments demonstrated that the injection brine by itself made the rock surface less oil-wet. The calcite surface became more water-wet as the 3-pentanone concentration increased;

however, the calcite wettability was more sensitive to the change in 3-pentanone concentration at low concentrations of 3-pentanone.

b. Huff-n-puff experiments demonstrated that the 3-pentanone solution increased the oil recovery from the tight rock matrix in comparison to the injection brine.
c. Improved oil recovery increased with increasing 3-pentanone concentration. Huff-n-puff with 2.85-wt% 3-pentanone solution showed the highest improved oil recovery, 28.6% of OOIP.
d. The huff-n-puff experiment with 1.07-wt% 3-pentanone solution showed the highest M_{P2}/M_{I3} value, 11.1. That is, the mass of oil produced was 11.1 times greater than the mass of 3-pentanone injected for this huff-n-puff experiment. The result indicates an optimal concentration in terms of efficiency of 3-pentanone, which gives the highest value of M_{P2}/M_{I3} for a given volume of the rock.

Credit author statement

Mingyuan Wang: Data curation; Formal analysis; Investigation; Methodology; Validation; Visualization; Writing – original draft. Gayan A. Abeykoon: Data curation; Formal analysis; Methodology. Francisco J. Argüelles-Vivas: Data curation; Investigation; Methodology. Ryosuke Okuno: Conceptualization; Formal analysis; Funding acquisition; Investigation; Methodology; Project administration; Resources; Supervision; Validation; Writing – review & editing.

Declaration of competing interest

The authors declare that they have no known competing financial interests or personal relationships that could have appeared to influence the work reported in this paper.

Acknowledgment

Ryosuke Okuno holds the Pioneer Corporation Faculty Fellowship in Petroleum Engineering at The University of Texas at Austin.

Nomenclature

Roman Symbols

b	fracture aperture, m
d	core diameter, m
D	relative contribution of a component to displacing oil in the matrix
F	apparent imbibed fraction
k	permeability, darcies
M	mass, kg
V	volume, m^3

Subscripts

e	effective
i	index for pseudo component
I	injected
f	fracture
m	matrix
P	produced
t	transfer

Abbreviations

3pIB	3-pentanone solution in injection brine
3pRB	1.1-wt% 3-pentanone solution in reservoir brine
IB	injection brine
IFT	interfacial tension
LSW	low-salinity water
OOIM	original oil volume in matrix
PTFE	Polytetrafluoroethylene
PV	pore volume
RB	reservoir brine
^{1}H NMR	proton nuclear magnetic resonance
XRD	X-ray diffraction analysis

References

Alfarge, D., Wei, M., Bai, B., 2017. IOR methods in unconventional reservoirs of north America: comprehensive review. In: Presented at SPE Western Regional Meeting, Bakersfield, California, USA, 23-27 April. https://doi.org/10.2118/185640-MS. SPE-185640-MS.

Alharthy, N., Teklu, T., Kazemi, H., Graves, R., Hawthorne, S., Braunberger, J., Kurtoglu, B., 2015. Enhanced oil recovery in liquid-rich shale reservoirs: laboratory to field. In: Presented at SPE Annual Technical Conference and Exhibition, Houston, Texas, USA, 28-30 September. https://doi.org/10.2118/175034-MS. SPE-175034-MS.

Alhashim, H.W., Zhang, F., Schechter, D.S., Chen, J., 2019. Investigation of the effect of pore size distribution on the produced oil from surfactant-assisted spontaneous imbibition in ULRs. In: Presented at the SPE Annual Technical Conference and Exhibition, Calgary, Alberta, Canada, 30 September – 2 October. https://doi.org/10.2118/195931-MS. SPE-195931-MS.

Alvarez, J.O., Neog, A., Jais, A., Schechter, D.S., 2014. Impact of surfactants for wettability alteration in stimulation fluids and the potential for surfactant EOR in unconventional liquid reservoirs. In: Presented at SPE Unconventional Resources Conference, the Woodlands, Texas, USA, 1-3 April. https://doi.org/10.2118/169001-MS. SPE-169001-MS.

Alvarez, J.O., Schechter, D.S., 2016. Wettability, oil and rock characterization of the most important unconventional liquid reservoirs in the United States and the impact on oil recovery. In: Presented at Unconventional Resources Technology Conference, San Antonio, Texas, USA, 1-3 August. https://doi.org/10.15530/URTEC-2016-2461651. URTEC-2461651-MS.

Alvarez, J.O., Schechter, D.S., 2017a. Wettability alteration and spontaneous imbibition in unconventional liquid reservoirs by surfactant additives. SPE Reservoir Eval. Eng. 20 (1), 107–117. https://doi.org/10.2118/177057-PA. SPE-177057-PA.

Alvarez, J.O., Schechter, D.S., 2017b. Improving oil recovery in the Wolfcamp unconventional liquid reservoir using surfactants in completion fluids. J. Petrol. Sci. Eng. 157, 806–815. https://doi.org/10.1016/j.petrol.2017.08.004.

Alvarez, J.O., Tovar, F.D., Schechter, D.S., 2018a. Improving oil recovery in the Wolfcamp reservoir by soaking/flowback production schedule with surfactant additives. SPE Reservoir Eval. Eng. 21 (4), 1083–1096. https://doi.org/10.2118/187483-PA. SPE-187483-PA.

Alvarez, J.O., Saputra, I.W.R., Schechter, D.S., 2018b. The impact of surfactant imbibition and adsorption for improving oil recovery in the Wolfcamp and Eagle Ford reservoirs. SPE J. 23 (6), 2103–2117. https://doi.org/10.2118/187176-PA. SPE-187176-PA.

Anderson, W.G., 1986. Wettability literature survey-Part 2: wettability measurement. J. Petrol. Technol. 38 (11), 1246–1262. https://doi.org/10.2118/13933-PA.

Argüelles-Vivas, F.J., Wang, M., Abeykoon, G.A., Okuno, R., 2020. Oil recovery from fractured porous media with/without initial water saturation by using 3-pentanone and its aqueous solution. Fuel 276, 118031. https://doi.org/10.1016/j.fuel.2020.118031.

Austad, T., Strand, S., Madland, M.V., Puntervold, T., Korsnes, R.I., 2008. Seawater in chalk: an EOR and compaction fluid. SPE Reservoir Eval. Eng. 11 (4), 648–654. https://doi.org/10.2118/118431-PA. SPE-118431-PA.

Barba, R.E., 2015. Liquids rich organic shale recovery factor Application. In: Presented at SPE Annual Technical Conference and Exhibition, Houston, Texas, USA, 28-30 September. https://doi.org/10.2118/174994-MS. SPE-174994-MS.

Bartley, J.P., Schwede, A.M., 1989. Production of volatile compounds in ripening kiwi fruit (*Actinidia chinensis*). J. Agric. Food Chem. 37, 1023–1025.

Berlioz, B., Cordella, C., Cavalli, J., Lizzani-Cuvelier, L., Loiseau, A., Fernandez, X., 2006. Comparison of the amounts of volatile compounds in French protected designation of origin virgin olive oils. J. Agric. Food Chem. 54 (26), 10092–10101.

Burrows, L.C., Haeri, F., Cvetic, P., Sanguinito, S., Shi, F., Tapriyal, D., Goodman, A., Enick, R.M., 2020. A literature review of CO2, natural gas, and water-based fluids for enhanced oil recovery in unconventional reservoirs. Energy Fuel. 34 (5), 5331–5380. https://doi.org/10.1021/acs.energyfuels.9b03658.

CAMEO Chemicals, https://cameochemicals.noaa.gov/chemical/8823 Accessed 23 March 2021.

Cavalli, J., Fernandez, X., Lizzani-Cuvelier, L., Loiseau, A., 2004. Characterization of volatile compounds of French and Spanish virgin olive oils by HS-SPME: identification of quality-freshness markers. Food Chem. 88, 151–157.

Chen, W., Schechter, D.S., 2021. Surfactant selection for enhanced oil recovery based on surfactant molecular structure in unconventional liquid reservoirs. J. Petrol. Sci. Eng. 196, 107702. https://doi.org/10.1016/j.petrol.2020.107702.

Clark, A.J., 2009. Determination of recovery factor in the Bakken formation, mountrail county, ND. In: Presented at SPE Annual Technical Conference and Exhibition, New Orleans, Louisiana, USA, 4-7 October. https://doi.org/10.2118/133719-STU. SPE-133719-STU.

Cronin, M., Emami-Meybodi, H., Johns, R.T., 2019. Diffusion-dominated proxy model for solvent injection in ultratight oil reservoirs. SPE J. 24 (2), 660–680. https://doi.org/10.2118/190305-PA. SPE-190305-PA.

Daubert, T.E., Danner, R.P., 1985. Data Compilation Tables of Properties of Pure Compounds. American Institute of Chemical Engineers, New York.

European Chemicals Bureau, 2007. IUCLID Dataset, 3-Pentanone (CAS # 99-22-0).

Ground Water Protection Council and ALL Consulting, 2009. Modern Shale Gas Development in the United States: A Primer. U.S. Department of Energy, Washington, DC.

He, K., Xu, L., 2017. Unique mixtures of anionic/cationic surfactants: a new approach to enhance surfactant performance in liquids-rich shale reservoirs. SPE Prod. Oper. 33 (2), 363–370. https://doi.org/10.2118/184515-PA. SPE-184515-PA.

Hoffman, B.T., Evans, J.G., 2016. Improved oil recovery IOR pilot projects in the Bakken formation. In: Presented at SPE Low Perm Symposium, Denver, Colorado, USA, 5-6 May. https://doi.org/10.2118/180270-MS. SPE-180270-MS.

Hoffman, B.T., 2018. Huff-N-Puff gas injection pilot projects in the Eagle Ford. In: Presented at SPE Canada Unconventional Resources Conference, Calgary, Alberta, Canada, 13-14 March. https://doi.org/10.2118/189816-MS. SPE-189816-MS.

Idstein, H., Schreier, P., 1985. Volatile constituents from guava (*Psidium guajava* L.) fruit. J. Agric. Food Chem. 33, 138–143.

Kathel, P., Mohanty, K.K., 2013. Wettability alteration in a tight oil reservoir. Energy Fuel. 27 (11), 6460–6468.

Kazempour, M., Kiani, M., Nguyen, D., Salehi, M., Bidhendi, M.M., Lantz, M., 2018. Boosting oil recovery in unconventional Resources utilizing wettability altering agents: successful translation from laboratory to field. In: Presented at SPE Improved Oil Recovery Conference, Tulsa, Oklahoma, USA, April. https://doi.org/10.2118/190172-MS. SPE-190172-MS.

Li, X., Teklu, T.W., Abass, H., Cui, Q., 2016. The impact of water salinity/surfactant on spontaneous imbibition through capillary and osmosis for unconventional IOR. In: Presented at SPE/AAPG/SEG Unconventional Resources Technology Conference, San Antonio, Texas, USA, August. https://doi.org/10.15530/URTEC-2016-2461736. URTEC-2461736-MS.

Liang, T., Zhao, X., Yuan, S., Zhu, J., Liang, X., Li, X., Zhou, F., 2020. Surfactant-EOR in tight oil reservoirs: current status and a systematic surfactant screening method with field experiments. J. Petrol. Sci. Eng. 196, 108097. https://doi.org/10.1016/j.petrol.2020.108097.

Liu, J., Sheng, J.J., Wang, X., Ge, H., Yao, E., 2019. Experimental study of wettability alteration and spontaneous imbibition in Chinese shale oil reservoirs using anionic and nonionic surfactants. J. Petrol. Sci. Eng. 175, 624–633.

Mejia, M., 2018. Experimental Investigation of Surfactant Flooding in Fractured Limestones. MS thesis. The University of Texas at Austin, Austin, Texas. December 2018.

Mullen, J., 2010. Petrophysical characterization of the Eagle Ford shale in south Texas. In: Presented at Canadian Unconventional Resources and International Petroleum Conference, Calgary, Alberta, Canada, 19-21 October. https://doi.org/10.2118/138145-MS. SPE-138145-MS.

Nelson, P.H., 2009. Pore-throat sizes in sandstones, tight sandstones, and shales. AAPG Bull. 93 (3), 329–340.

Nguyen, D., Wang, D., Oladapo, A., Zhang, J., Sickorez, J., Butler, R., Mueller, B., 2014. Evaluation of surfactants for oil recovery potential in shale reservoirs. In: Presented at SPE Improved Oil Recovery Symposium, Tulsa, Oklahoma, USA, 12-16 April. https://doi.org/10.2118/169085-MS. SPE-169085-MS.

Nishimura, O., Yamaguchi, K., Mihara, S., Shibamoto, T., 1989. Volatile constituents of guava fruits (*Psidium guajava* L.) and canned puree. J. Agric. Food Chem. 37, 139–142.

Pet'ka, J., Leitner, E., Parameswaran, B., 2012. Musk strawberries: the flavour of a formerly famous fruit reassessed. Flavour Fragrance J. 27 (4), 273–279.

PubChem, https://pubchem.ncbi.nlm.nih.gov/compound/Methane#section=Acute-Effects Accessed 23 March 2021.

Sheng, J.J., 2017. Critical review of field EOR projects in shale and tight reservoirs. J. Petrol. Sci. Eng. 159, 654–665. https://doi.org/10.1016/j.petrol.2017.09.022.

Shuler, P.J., Tang, H., Lu, Z., Tang, Y., 2011. Chemical process for improved oil recovery from bakken shale. In: Presented at Canadian Unconventional Resources Conference, Calgary, Alberta, Canada, 15-17 November. https://doi.org/10.2118/147531-MS. SPE-147531-MS.

Slatt, R.M., Galvis-Portillo, H., Becerra-Rondon, D., Ekwunife, I.C., Brito, R., Zhang, J., Molinares, C., Torres, E., Duarte, D., Milad, B., 2018. Outcrop and subsurface geology applied to drilling, sweep spot and target zone detection of resource shales: the woodford example. In: Presented at the Unconventional Resources Technology Conference, Houston, Texas, USA, 23-25 July. https://doi.org/10.15530/URTEC-2018-2893838. URTEC-2893838-MS.

Teklu, T.W., Li, X., Zhou, Z., Alharthy, N., Wang, L., Abass, H., 2018. Low-salinity water and surfactants for hydraulic fracturing and EOR of shales. J. Petrol. Sci. Eng. 162, 367–377. https://doi.org/10.1016/j.petrol.2017.12.057.

Tovar, F.D., Barrufet, M.A., Schechter, D.S., 2018. Gas injection for EOR in organic rich shales. Part I: operational philosophy. In: Presented at the SPE Improved Oil Recovery Conference, Tulsa, Oklahoma, USA, 14-18 April. https://doi.org/10.2118/190323-MS. SPE-1903232-MS.

Vacher, J., Deraedt, R., Benzoni, J., 1973. Compared effects of two beryllium salts (soluble and insoluble): toxicity and blockade of the reticuloendothelial system. Toxicol. Appl. Pharmacol. 24, 497–506.

Valluri, M.K., Alvarez, J.O., Schechter, D.S., 2016. Study of the rock/fluid interactions of sodium and calcium brines with ultra-tight rock surfaces and their impact on improving oil recovery by spontaneous imbibition. In: Presented at the SPE Low Perm Symposium, Denver, Colorado, USA, May. https://doi.org/10.2118/180274-MS. SPE-180274-MS.

Wang, D., Butler, R., Zhang, J., Seright, R., 2012. Wettability survey in bakken shale with surfactant-formulation imbibition. SPE Reservoir Eval. Eng. 15 (6), 695–705. https://doi.org/10.2118/153853-PA. SPE-153853-PA.

Wang, L., Tian, Y., Yu, X., Wang, C., Yao, B., Wang, S., Winterfeld, P.H., Wang, X., Yang, Z., Wang, Y., Cui, J., Wu, Y., 2017. Advances in improved/enhanced oil recovery technologies for tight and shale reservoirs. Fuel 210, 425–445.

Wang, M., Abeykoon, G.A., Argüelles Vivas, F.J., Okuno, R., 2019. Ketone solvent as a wettability modifier for improved oil recovery from oil-wet porous media. Fuel 258, 116195. https://doi.org/10.1016/j.fuel.2019.116195.

Wang, M., Baek, K., Abeykoon, G.A., Argüelles Vivas, F.J., Okuno, R., 2020a. Comparative study of ketone and surfactant for enhancement of water imbibition in fractured porous media. Energy Fuel. 34 (5), 5159–5167. https://doi.org/10.1021/acs.energyfuels.9b03571.

Wang, M., Abeykoon, G.A., Argüelles Vivas, F.J., Okuno, R., 2020b. Aqueous solution of ketone solvent for enhanced water imbibition in fractured carbonate reservoirs. SPE J. 25 (5), 2694–2709. https://doi.org/10.2118/200340-PA.

Zeng, T., Miller, C.S., Mohanty, K.K., 2018. Application of surfactants in shale chemical EOR at high temperatures. In: Presented at the SPE Improved Oil Recovery Conference, Tulsa, Oklahoma, USA, 14-18 April. https://doi.org/10.2118/190318-MS. SPE-190318-MS.

Zeng, T., Kim, K.T., Werth, C.J., Katz, L.E., Mohanty, K.K., 2020. Surfactant adsorption on shale samples: experiments and an additive model. Energy Fuel. 34 (5), 5436–5443. https://doi.org/10.1021/acs.energyfuels.9b04016.

Zhang, J., Wang, D., Butler, R., 2013. Optimal salinity study to support surfactant imbibition into the bakken shale. In: Presented at the SPE Unconventional Resources Conference Canada, Calgary, Alberta, Canada, November. https://doi.org/10.2118/167142-MS. SPE-167142-MS.